Dynamics of nonspherical compound capsules in simple shear flow

Zheng Yuan Luo and Bo Feng Bai

Citation: Physics of Fluids **28**, 101901 (2016); doi: 10.1063/1.4965251
View online: http://dx.doi.org/10.1063/1.4965251
View Table of Contents: http://scitation.aip.org/content/aip/journal/pof2/28/10?ver=pdfcov
Published by the AIP Publishing

PHYSICS OF FLUIDS **28**, 101901 (2016)

Dynamics of nonspherical compound capsules in simple shear flow

Zheng Yuan Luo and Bo Feng Bai[a)]
State Key Laboratory of Multiphase Flow in Power Engineering, Xi'an Jiaotong University, Xi'an 710049, China

(Received 22 April 2016; accepted 6 October 2016; published online 20 October 2016)

The dynamics of an initially ellipsoidal compound capsule in a simple shear flow is investigated numerically using a three-dimensional front-tracking finite-difference model. Membrane bending resistance is included based on Helfrich's energy function besides the resistances against shear deformation and area dilatation governed by the constitutive law of Skalak *et al*. In this paper, we focus specifically on how the presence of a spherical inner capsule and its size affects the characteristics and transition of various dynamical states of nonspherical compound capsules (i.e., the outer capsule). Significant differences in the dynamical characteristics are observed between compound capsules and homogeneous capsules in both qualitative and quantitative terms. We find the transition from swinging to tumbling can occur at vanishing viscosity mismatch through increasing the inner capsule size alone to a critical value regardless of the initial shape of the nonspherical compound capsule (i.e., prolate or oblate). Besides, for compound capsules with viscosity mismatch, the critical viscosity ratio for the swinging-to-tumbling transition remarkably decreases by increasing the inner capsule size. It is thus concluded that the inner capsule size is a key governing parameter of compound capsule dynamics apart from the capillary number, aspect ratio, and viscosity ratio that have been long identified for homogeneous capsules. Further, we discuss the mechanisms underlying the effects of the inner capsule on the compound capsule dynamics from the viewpoint of the effective viscosity of internal fluid and find that the effects of the inner capsule on compound capsule dynamics are qualitatively similar to that of increasing the internal viscosity on homogeneous capsule dynamics. However, in quantitative terms, the compound capsule cannot be viewed as a homogeneous capsule with higher viscosity as obvious inhomogeneity in fluid stress distribution is induced by the inner membrane. *Published by AIP Publishing.* [http://dx.doi.org/10.1063/1.4965251]

I. INTRODUCTION

Capsules are small liquid droplets surrounded by thin membranes possessing complex mechanics, such as shear elasticity and bending resistance. They have been widely used for numerous applications in bioengineering, pharmaceutical, and cosmetic industries (e.g., encapsulation and transport of active agents)[1–4] and have also been employed as models for biological cells (e.g., red blood cells).[1–3] The release of substances from capsules by breaking or diffusion heavily depends on the stress and strain states in the capsule membrane, which is affected by the dynamical characteristics of whole capsules in shear flow. Further, flow rheology of capsule suspensions (e.g., biological cell suspensions and artificial capsule suspensions) is also significantly influenced by single object dynamics. Therefore, to study the dynamic motion of single capsules in shear flow is helpful for technically controlling their functions and is also fundamental for

a)Author to whom correspondence should be addressed. Electronic mail: bfbai@mail.xjtu.edu.cn

understanding flow behaviors of capsule suspensions. Though studies on the dynamics of single capsules in shear flow have attracted much research attention for decades, there remain many unknown issues due to the complexities in membrane mechanics, fluid mechanics, and their interactions.

Various types of dynamic motion have been observed for capsules suspended in simple shear flow.[3,5] Initially spherical capsules always exhibit a steady tank-treading motion.[5] In this mode, the capsule is deformed by the elongational part of the simple shear flow and maintains a stationary shape with a constant inclination to the flow direction, while its membrane rotates like a tank-tread due to the rotational part of the simple shear flow. With higher surface-to-volume ratio, initially non-spherical shapes are common in biological capsules (e.g., biconcave-shaped red blood cells) and artificial capsules in engineering applications. The non-sphericity confers shape memory effect[6,7] to the capsules owing to the shear elasticity of their membranes; as a consequence, the capsules exhibit a swinging motion (i.e., a tank-treading motion accompanying the periodically oscillatory inclination). When the flow shear rate decreases to very low values, the swinging-to-tumbling transition occurs (i.e., tumbling is a rigid-body-like rotation),[7–9] as the external flow cannot provide sufficient energy for the membrane tank-treading any longer. Extensive studies have reported that the increase of the non-sphericity or the membrane shear elasticity promotes the tumbling motion due to the pronounced shape memory effect.[8–11] The dynamic motion of capsules is also affected by the bending resistance of their membranes.[12–15] It is noteworthy that the swinging-to-tumbling transition can be induced by increasing the viscosity contrast of the internal to external fluids or the membrane viscosity.[10,11,14,16–18] It is because the viscous dissipation increases with the viscosity of the internal fluid and the capsule membrane; as a result, the effective energy provided by the external flow to overcome the energy barrier from the shape memory effect is reduced.

The above-mentioned previous studies mainly focus on the dynamics of homogeneous capsules which consist of an elastic membrane enclosing a homogeneous fluid. Notably, there are cases of compound capsules (i.e., capsules containing smaller inclusions), such as white blood cells, circulating tumor cells, parasite-infected red blood cells, and artificial capsules fabricated from multiple emulsions.[19] The presence of smaller inclusions induces additional complexity to the capsule dynamics due to the hydrodynamic interaction between the capsule membrane and inclusions. Evidently, in the case of liquid drops with compound structures, the inclusion significantly affects their deformation and breakup.[20–24] A limited number of studies have demonstrated that internal structures cause more complex dynamical behaviors for vesicles (i.e., liquid drops surrounded by membranes with bending and area-dilatation resistances but without shear elasticity). Experimental studies[25–27] show that compound vesicles exhibit much richer dynamics than homogeneous vesicles, but neither the inclusion-induced transition nor a phase diagram of dynamical states is obtained due to the complexities in fabricating compound vesicles and controlling a large number of related parameters. By using small-deformation analysis and two-dimensional (2D) boundary integral simulations, Veerapaneni *et al.*[28] present the tank-treading-to-tumbling transition of compound vesicles enclosing solid particles induced by increasing the particle size alone. The same phenomenon is also observed for compound vesicles enclosing deformable vesicles in the 2D lattice Boltzmann simulations by Kaoui *et al.*[29] Nevertheless, the dynamics of compound capsules are largely unexplored. For one thing, there are large differences between the dynamics of capsules and vesicles due to their different membrane mechanics. For another, the 2D simulation or theoretical analysis used in previous studies is not capable of quantitatively capturing the dynamical behavior of capsules or vesicles with large deformations in the actual 3D environments.[1–3] Apparently, a comprehensive investigation into the dynamics of compound capsules is still lacking, particularly into the altered dynamical characteristics induced by the inner capsule, which is the main objective of the present study.

Very recently, we developed a 3D model based on a front-tracking finite-difference method and systematically investigated the deformation of spherical compound capsules in simple shear flow.[30] The present work is an extended one for a study on the dynamics of nonspherical compound capsules, since previous studies on homogeneous capsules have shown that initially nonspherical capsules exhibit dynamic motions quite different from spherical ones.[3,5] In this study, of particular

interest is how the presence of the inner capsule and its size affects the characteristics of various dynamical states of compound capsules and the transition between these dynamical states. On the basis of the front-tracking finite-difference model that we have developed in our previous study, the bending resistance of membranes is included apart from the shear elasticity and area dilatation. We find that compound capsules can exhibit both swinging and tumbling at vanishing viscosity mismatch and the transition between these two dynamical states can be induced by changing the inner capsule size alone. Further, the mechanisms underlying the effects of the inner capsule on the compound capsule dynamics are discussed.

II. PROBLEM STATEMENT AND NUMERICAL METHOD

We consider an initially ellipsoidal compound capsule suspended in a simple shear flow $\boldsymbol{u} = [\gamma z, 0, 0]$, where γ is the shear rate (Figure 1). The compound capsule consists of a spherical capsule (i.e., the inner capsule) enclosed by an ellipsoidal capsule outside (i.e., the outer capsule). The ellipsoidal shape of the outer capsule is denoted by the length of the revolution axis $2a$ and the length of the two orthogonal axes $2b$. The compound capsule is prolate with the aspect ratio $a/b > 1$, unless stated otherwise. The fluids surrounding the compound capsule between the two membranes and inside the inner capsule are all incompressible and Newtonian. Their viscosities are μ, $\lambda\mu$ and $\lambda^{in}\lambda\mu$, respectively, where λ and λ^{in} are viscosity contrasts. Both the inner and outer membranes are considered as 2D elastic interfaces possessing resistances against the shear, area-dilatation, and bending. For the shear and area-dilatation resistances, we use the SK constitutive law[31]

$$W_e = \frac{E_s}{4}\left({\lambda_1}^4 + {\lambda_2}^4 - 2{\lambda_1}^2 - 2{\lambda_2}^2 + 2\right) + \frac{E_a}{4}\left({\lambda_1}^2{\lambda_2}^2 - 1\right)^2, \tag{2.1}$$

where λ_1 and λ_2 are the principal in-plane stretch ratios, and E_s and E_a are the moduli of shear and area-dilatation. For the bending resistance, we use Helfrich's bending energy function[32,33]

$$W_b = \frac{E_b}{2}\int_S (2H - C_0)^2 dS. \tag{2.2}$$

Here, E_b is the bending modulus, and H and C_0 are the mean and spontaneous curvatures. Since the effects of bending stiffness on capsule dynamics have been investigated fully in previous studies;[12,34,35] in this paper, we only add a constant bending resistance to avoid buckling instability. It is noteworthy that different choices of the constitutive model used for the membrane

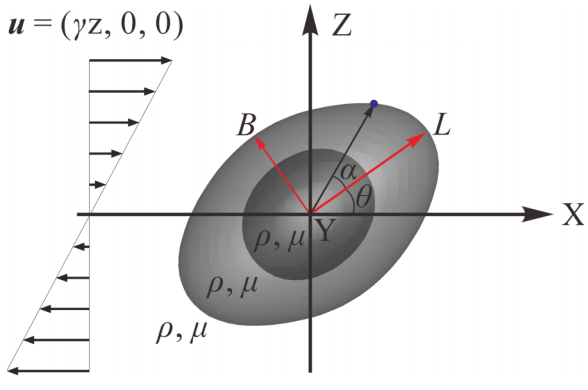

FIG. 1. Schematic illustrating an initially ellipsoidal compound capsule in simple shear flow. The compound capsule consists of a prolate/oblate capsule containing a smaller spherical capsule inside. The orientation angle θ between the major axis L and the X-axis (i.e., the flow direction) is used to characterize the orientation dynamics of the capsule. The deformation index $D = (L - B)/(L + B)$ is used to characterize the shape deformation. The phase angle α of a fixed point on the membrane is used to characterize the rotation of the capsule membrane.

mechanics may result in different findings regarding the whole-capsule dynamics.[36] In the present study, we employ the Skalak and Helfrich models since they have been widely used in previous studies on the dynamics of capsules, vesicles, and biological cells.[2,3,37] However, other constitutive laws can be easily implemented into the present method as shown in our previous work.[30]

In our earlier publications,[30,38,39] we have developed a 3D numerical model to simulate the dynamics of homogeneous capsules in shear flow and have extended it to study the deformation of spherical compound capsules. We further develop the 3D model to study the dynamics of nonspherical compound capsules in the present study. In the present model, a front-tracking finite-difference method is used to solve the flow fields inside and outside the capsule and a finite-element method is used to solve the elastic tensions in the capsule membrane. The numerical method is briefly described in this section, and more details of the numerical procedure and model validation can be found in the Refs. 30, 38, and 39.

In the front-tracking method,[40–42] the flow field is obtained by solving the continuity and Navier–Stokes (NS) equations on a structured Eulerian grid system

$$\begin{gathered}\nabla \cdot \boldsymbol{u} = 0, \\ \frac{\partial (\rho \boldsymbol{u})}{\partial t} + \nabla \cdot (\rho \boldsymbol{u}\boldsymbol{u}) = -\nabla p + \mu \nabla^2 \boldsymbol{u} + \int_S \boldsymbol{f}' \delta (\boldsymbol{x} - \boldsymbol{x}')\, d\boldsymbol{x}'.\end{gathered} \tag{2.3}$$

Here, $\boldsymbol{u}$ is the velocity vector, ρ, t, and p are the fluid density, time, and pressure, respectively, $\boldsymbol{f}'$ is the elastic tension in the capsule membrane, δ is the 3D Dirac-Delta function, and $\boldsymbol{x}'$ and $\boldsymbol{x}$ are the position vectors of points on the membrane and in the surrounding fluid, respectively. The capsule membrane is tracked by a set of Lagrangian points and triangular elements, thus the elastic tension $\boldsymbol{f}'$ can be computed via the constitutive laws (e.g., Equations (2.1) and (2.2)) using a finite-element method for curved elastic membranes.[43] When the viscosities of the fluids inside and outside the capsule are different, an indicator function $I(\boldsymbol{x})$ is used to distinguish the three fluids. For example, $I = 0$, 1, and 2 represent the fluid surrounding the compound capsule between the two membranes and inside the inner capsule, respectively. Accordingly, the fluid viscosity can be calculated by

$$\mu (\boldsymbol{x}) = \begin{cases} \mu + \mu (\lambda - 1) I (\boldsymbol{x}), & \text{for } 0 \le I (\boldsymbol{x}) \le 1, \\ \lambda \mu + \lambda \mu \left(\lambda^{in} - 1\right) (I (\boldsymbol{x}) - 1), & \text{for } 1 < I (\boldsymbol{x}) \le 2. \end{cases} \tag{2.4}$$

The indicator function can be constructed from the Dirac-Delta function.

The compound capsule is placed in the center of the computational domain with a size of $L_x \times L_y \times L_z = 8R \times 5R \times 8R$, where R is the radius of a sphere having the same volume as the outer capsule. The revolution axis is initially placed in the shear plane and it remains in this position due to the symmetry of the whole flow system. The governing equations are recast into dimensionless form through scaling lengths by R, time by γ^{-1}, and velocity by γR. The dimensionless parameters governing the compound capsule dynamics mainly include the Reynolds number $Re = \rho \gamma R^2/\mu$ and the capillary number $Ca = \mu \gamma R/E_s{}^{out}$ based on the parameters of the outer capsule, the ratio of the shear moduli of the outer to the inner membrane $\kappa = E_s{}^{out}/E_s{}^{in}$, the ratio of the area-dilatation modulus and the bending modulus to the shear modulus (i.e., $C = E_a/E_s$ and $E_b{}^* = E_b/R^2 E_s$), the viscosity ratios λ and λ^{in}, the aspect ratio of the compound capsule a/b and the volume ratio of the inner to the outer capsule ϕ. As presented in previous studies on the dynamics of homogeneous capsules, Ca, a/b, and λ are the key governing parameters that have been studied most extensively; thus in this paper, we address the dynamics of compound capsules under varying Ca, a/b, λ and λ^{in} ($\lambda = \lambda^{in} = 1$ unless stated otherwise), and volume ratio ϕ. Re is set at 0.1 to neglect the effect of fluid inertia.[30,38] C and $E_b{}^*$ are set to 1 and 0.01 for both the inner and outer membranes, which are used in previous studies on homogeneous capsules.[16,44,45] Note that C has to be much higher than 1 when we apply the present model for red blood cell membranes. The mechanical parameters are kept the same (i.e., κ is held constant at 1) for the inner and outer membranes for simplicity. However, we note that changes in C, $E_b{}^*$, and κ can also induce quantitative variations in the dynamical characteristics of compound capsules.

The shape deformation and orientation dynamics of the compound capsule are analyzed using the Taylor parameters, i.e., the deformation index D and the orientation angle θ (Figure 1). More details of the problem setup, the parameters used, the numerical convergence tests, and the model validation of membrane shear elasticity and area dilatation can be found in our previous study on the deformation of spherical compound capsules.[30] The validation of the bending resistance modeling is also available in our earlier study on the dynamics of nonspherical homogeneous capsules.[38]

III. PROLATE COMPOUND CAPSULES WITH $\lambda = \lambda^{in} = 1$

We first present the dynamics of the compound capsules containing the inclusions with different sizes and compare with the dynamics of the homogeneous capsules. The time evolutions of the capsule shape, the orientation angle θ and the phase angle α of a fixed membrane point are presented in Figure 2 for two compound capsules with $\phi = 0.05$ and 0.2 ($Ca = 0.1$ and $a/b = 1.32$), respectively. For the comparison purpose, corresponding parameters of a homogeneous capsule with the same Ca and a/b are also presented. As shown in Figure 2(a), the homogeneous capsule exhibits the swinging motion, as θ oscillates over time about a positive value (Figure 2(d)) and the membrane rotates like a tank-tread at the same time (Figure 2(e)). This swinging motion has also been observed in previous simulations by other researchers.[10,13,46] Notably, the compound capsule with $\phi = 0.05$ also exhibits the swinging mode (Figures 2(b), 2(d), and 2(e)). However, at $\phi = 0.2$, the compound capsule exhibits the tumbling state (Figures 2(c)–2(e)). In this dynamical state, the orientation angle periodically oscillates from $\theta = +\pi/2$ to $\theta = -\pi/2$ (Figure 2(d)). Besides, the

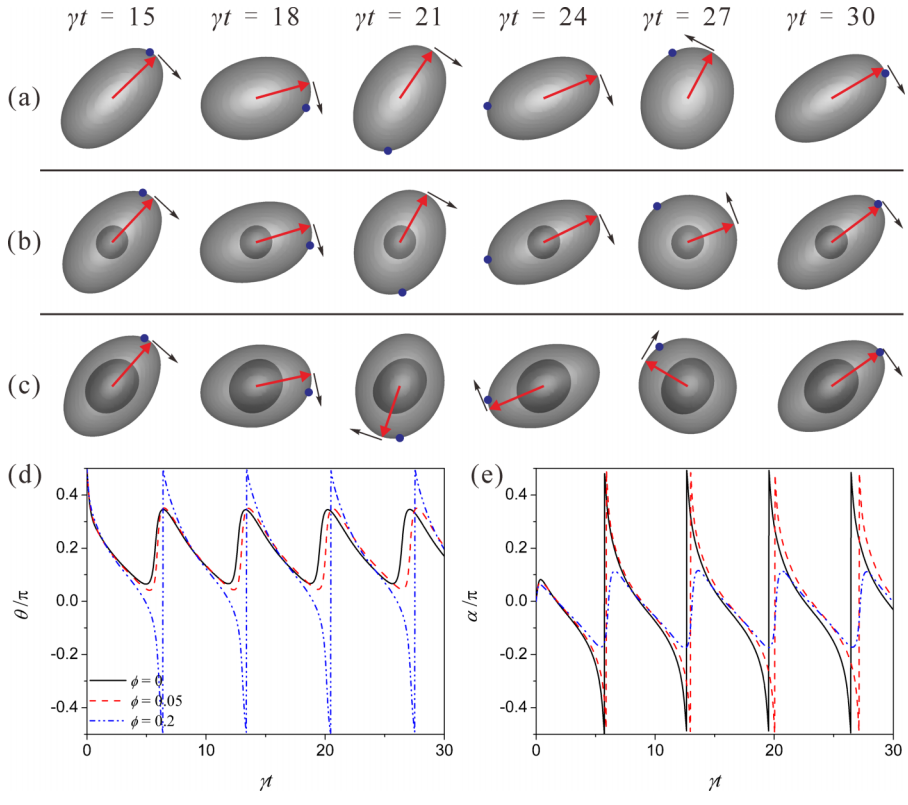

FIG. 2. Orientation dynamics of initially prolate capsules containing inner capsules with different volume ratios. The shape evolutions of capsules with $Ca = 0.1$ and $a/b = 1.32$ are presented at $\phi =$ (a) 0, (b) 0.05, and (c) 0.2. Arrows inside and outside the capsule indicate the major-axis and the rotation direction, respectively. (d) and (e) are the time evolutions of the orientation angle θ and phase angle α for the three cases presented in (a)–(c). The capsule exhibits the swinging motion at $\phi = 0$ and 0.05 and exhibits the tumbling motion at $\phi = 0.2$.

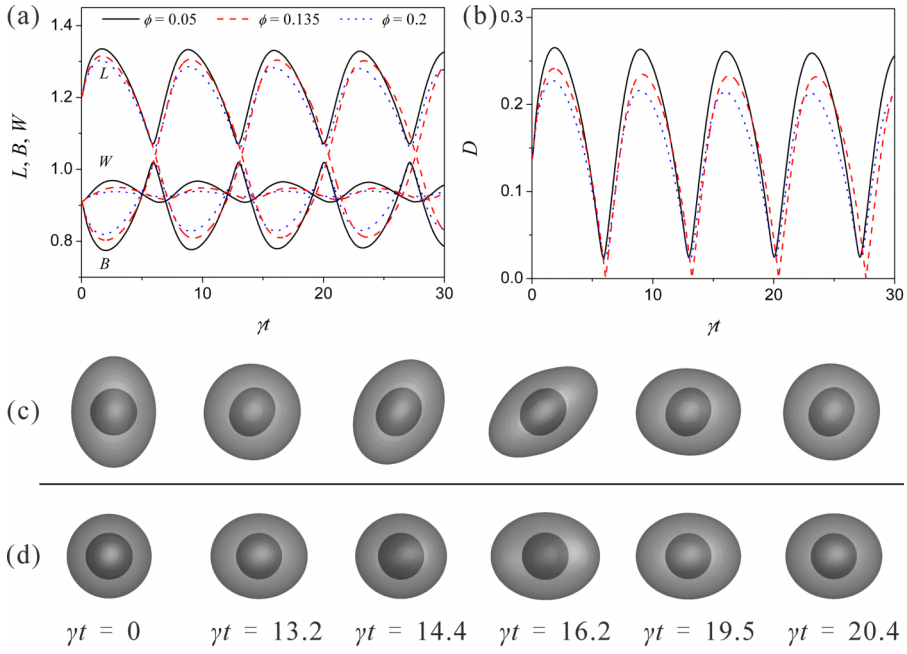

FIG. 3. Shape deformations of compound capsules ($Ca = 0.1$ and $a/b = 1.32$) containing inner capsules with different volume ratios ($\phi = 0.05$, 0.135, and 0.2). (a) Time evolutions of the semimajor axis L, the semiminor axis B and the half axis length W in the vorticity direction. (b) Deformation index D versus time. (c) Side view and (d) top view of instantaneous shapes of the compound capsule with $\phi = 0.135$.

membrane no longer rotates about the capsule center but oscillates back and forth about the capsule major axis, which is indicated by the oscillation of the phase angle about $\alpha = 0$ with an amplitude smaller than $\pi/2$ (Figure 2(e)). Previous theoretical analysis and 2D simulations[28,29] demonstrate that compound vesicles present tumbling at high volume ratio of inclusions, but at low volume ratios they present the tank-treading state.

The transient deformation is then analysed by presenting the time evolutions of the lengths of three principal axes (i.e., the semimajor axis L and the semiminor axis B in the shear plane and the half axis length W in the vorticity direction) and the deformation index D in Figure 3 for three compound capsules with $\phi = 0.05$, 0.135, and 0.2, respectively. The compound capsule either in the swinging regime ($\phi = 0.05$) or in the tumbling regime ($\phi = 0.2$) shows significant deformation oscillating periodically, which is indicated by the oscillations of L, B, W, and D with large amplitudes (Figures 3(a) and 3(b)). In each specific oscillation period, the capsule shape changes continuously between a prolate shape and an oblate shape with the revolution axis in the shear plane and in the vorticity direction (Figures 3(c) and 3(d)), respectively, particularly for the compound capsule at the swinging-to-tumbling transition ($\phi = 0.135$). This deformation behaviour is similar to that of the homogeneous capsules at the swinging-to-tumbling transition induced by changing viscosity contrast.[10,13] Notably, changing the inner capsule size significantly affects the deformation of the compound capsule. For example, as ϕ increases from 0.05 to 0.2, the oscillation amplitude of W decreases; the maximum value of L decreases but the minimum value of B increases leading to a decrease of the maximum value of D (Figure 3(a) and 3(b)). Specifically, the minimum value of D at $\phi = 0.135$ is nearly zero when the compound capsule is nearly at the swinging-to-tumbling transition (Figure 3(b)).

Next, we perform a systematic analysis of the effects of the inner capsule on the dynamical characteristics of the compound capsules in the swinging or tumbling regime. To study the effects of the inner capsule on the orientation dynamics of the compound capsules, the time-average value θ_{av} and the minimum value θ_{min} of the orientation angle are plotted as functions of the volume ratio ϕ of the inner capsule in Figure 4 for different values of Ca and a/b. When the compound capsule is in the swinging regime (e.g., $Ca = 0.2$ in Figure 4(a) and $a/b = 1.3$ in Figure 4(b)),

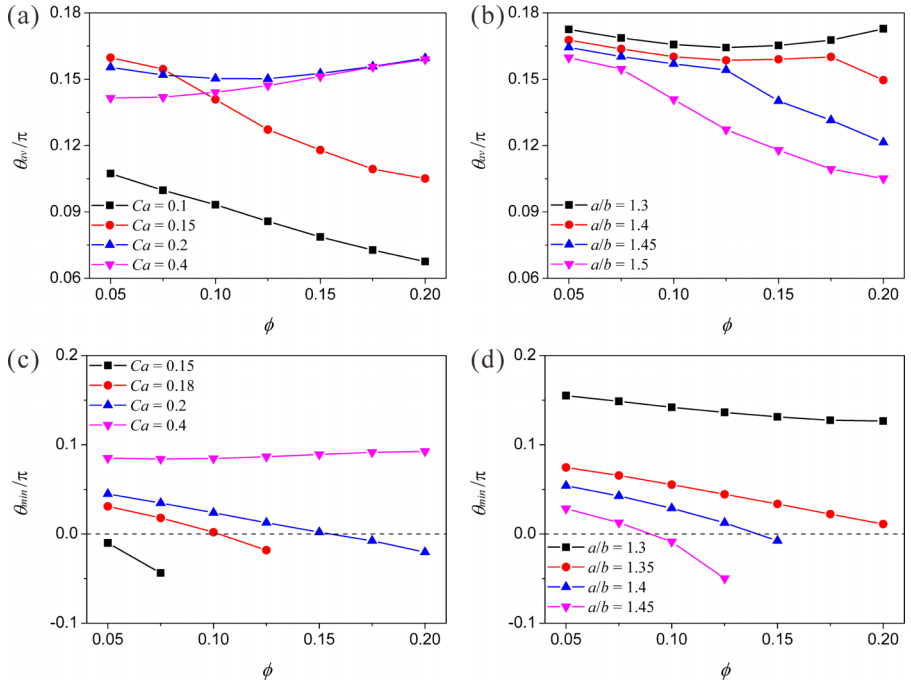

FIG. 4. The effect of the inner capsule on the orientation dynamics of compound capsules. The time-average value θ_{av} and the minimum value θ_{min} of the orientation angle are plotted as functions of ϕ. (a) and (c) are for capsules with $a/b = 1.5$ at different Ca. (b) and (d) are for capsules with $Ca = 0.15$ at different a/b. $\theta_{av} = \int_T \theta dt/T$, where T is the oscillation period.

θ_{av} first decreases and then increases as ϕ increases. At the swinging-to-tumbling transition, θ_{av} shows a sharp decrease tendency (e.g., $Ca = 0.15$ in Figure 4(a) and $a/b = 1.4$–1.5 in Figure 4(b)). Note that θ_{av} is not zero even though the compound capsule is in the tumbling regime (e.g., $Ca = 0.1$ in Figure 4(a)). It is because the significant deformation induces an asymmetry in θ about zero, which is also observed for homogeneous capsules.[10] In previous theoretical analyses and 2D simulations,[28,29] the transition from tank-treading to tumbling for compound vesicles occurs when $\theta = 0$. However, in our 3D simulations, the swinging-to-tumbling transition for compound capsules occurs when $\theta_{av} > 0$ and $\theta_{min} < 0$. As ϕ increases, θ_{min} decreases in most cases of Ca and a/b (Figures 4(c) and 4(d)). It is worthy of mention that θ_{min} may decrease to be lower than zero near the swinging-to-tumbling transition (Figures 4(c) and 4(d)), which means that the orientation angle alternates between positive and negative periodically. Bagchi and Kalluri[10] demonstrate numerically that θ_{min} of the homogeneous capsules can also decrease to be negative with increasing viscosity ratio and they categorize this motion as a vacillating-breathing motion. Our present work shows that by increasing the inner capsule size alone, the dynamical state of compound capsules can also change from swinging to tumbling through vacillating-breathing at a vanishing viscosity ratio.

To study the effects of the inner capsule on the shape deformation of the compound capsule, the time-average value D_{av} and the minimum value D_{min} of the deformation index are plotted as functions of the volume ratio ϕ in Figure 5. As ϕ increases, D_{av} decreases monotonically in all the cases shown in Figures 5(a) and 5(b), regardless of the regime that the compound capsule is in the swinging or tumbling regime. This tendency of D_{av} versus ϕ is similar to that of the spherical compound capsules demonstrated in our previous work, which results from the increasing hydrodynamic interaction between the two membranes.[30] The influence of the inner capsule on the minimum deformation is more complex (Figures 5(c) and 5(d)). As ϕ increases, D_{min} decreases in the swinging regime (e.g., $Ca = 0.2$–0.3 in Figure 5(c)) but increases in the tumbling regime (e.g., $Ca = 0.1$ in Figure 5(c)). Particularly, when the capsule approaches the swinging-to-tumbling transition, as ϕ increases, D_{min} linearly decreases to zero in the swinging regime and then linearly

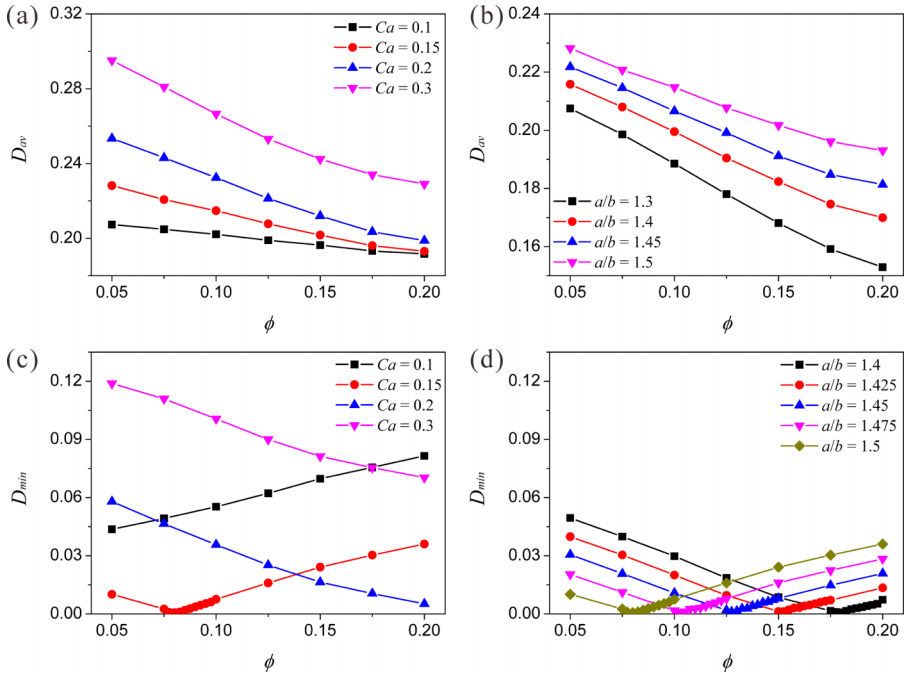

FIG. 5. The effect of the inner capsule on the shape deformation of compound capsules. The time-average value D_{av} and the minimum value D_{min} of the deformation index are plotted as functions of ϕ. (a) and (c) are for capsules with $a/b = 1.5$ at different Ca. (b) and (d) are for capsules with $Ca = 0.15$ at different a/b.

increases from zero in the tumbling regime (Figure 5(d) and $Ca = 0.15$ in Figure 5(c)). It means that the swinging-to-tumbling transition induced by increasing the inner capsule size occurs when the compound capsule shape in the shear plane is circular. Walter *et al.*[13] observe that the homogeneous capsules at the swinging-to-tumbling transition induced by increasing the viscosity ratio present a circular shape in the shear plane. Our 3D simulations show that the compound capsule in 3D is ellipsoidal at the transition with a circular shape in the shear plane. For example, the capsule is an oblate ellipsoid with the revolution axis in the vorticity direction as shown in Figures 3(c) and 3(d).

As indicated in Figures 4 and 5, the inner capsule has significant influences on the dynamical characteristics of both the swinging and tumbling motions of compound capsules. Next, we present how the inner capsule size affects the swinging-to-tumbling transition. The phase diagram for the occurrence of various dynamical states is presented in the Ca–ϕ and a/b–ϕ planes (Figure 6). The tank-treading motion with stationary orientation angles is not observed in both phase diagrams, while it is predicted in previous theoretical analyses and 2D simulations for compound vesicles.[28,29] Instead, we observe the swinging motion with oscillating orientation angles and the vacillating-breathing motion (i.e., swinging with $\theta_{min} < 0$) at relatively low values of ϕ. Apart from Figures 2 and 4, the phase diagrams in Figure 6 again indicate that the dynamical state of compound capsules can be altered at vanishing viscosity mismatch from swinging to tumbling by only increasing ϕ. Certainly, the swinging-to-tumbling transition can be also induced by decreasing Ca or increasing a/b alone, which is similar to the case for homogeneous capsules.[10,17] As ϕ increases, the critical Ca for the transition increases but the critical a/b decreases both in an approximately linear tendency. Notably, the linear tendencies are observed in the present range of the volume ratio considered in this study, but there is high possibility to observe non-linear tendencies at higher values of the volume ratio, which needs to be studied in future works.

In Figure 7, the critical value of the inner capsule volume ratio ϕ_c for the swinging-to-tumbling transition of compound capsules is plotted versus the reduced volume υ for different values of Ca. The prediction of small deformation theory by Veerapaneni *et al.*[28] for compound vesicles enclosing

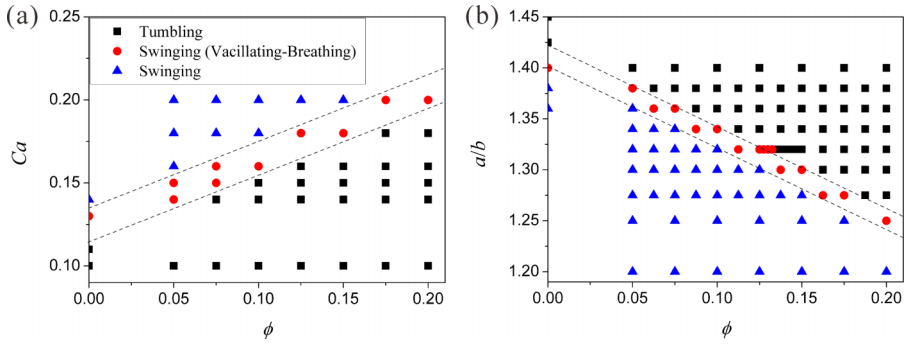

FIG. 6. Phase diagrams for the occurrence of different dynamical states (a) as a function of ϕ and Ca at $a/b = 1.5$ and (b) as a function of ϕ and a/b at $Ca = 0.1$. The vacillating-breathing motion is characterized as the swinging motion with $\theta_{min} < 0$.

a rigid particle is also presented. The reduced volume represents the ratio of the capsule volume to that of a sphere having the same surface area as the capsule, which is widely used to describe the shape effect in the study on homogeneous capsules/vesicles.[39,47] The increase of ϕ_c with increasing υ is observed in both previous theoretical and our numerical results. Note that in theory the dynamical state transition (i.e., ϕ_c) is considered to be independent of the capillary number, but our numerical simulations demonstrate strong dependence of ϕ_c on Ca. It is found that ϕ_c significantly increases with Ca increasing. Previous studies on homogeneous capsules indicate that the influence of the shape deformation on the capsule dynamics is significant at high Ca.[3,10,13] The variations of ϕ_c with Ca and υ indicates that it is more difficult for compound capsules with higher deformability or sphericity to exhibit tumbling, which is similar with the observation for homogeneous capsules.[3,5] Notably, when υ deviates from unity to lower values (i.e., the initial shape of the compound capsule is more discrepant from the sphere), ϕ_c obtained by our numerical simulations is much lower than that from the small deformation theory. It is because the capsule shape is considered as quasi-spherical in the small deformation theory that underestimates the effect of the non-sphericity of the shape. These results further suggest that small deformation theories compared to numerical simulations are only applicable for the study on the dynamics of quasi-spherical capsules with negligible deformation.

Recent studies have shown that off-plane motion is also important for non-spherical capsules;[45,46,48] thus we examine the effects of the compound structure on the dynamics of non-spherical capsules with the revolution axis initially off the shear plane. Within the parameter range

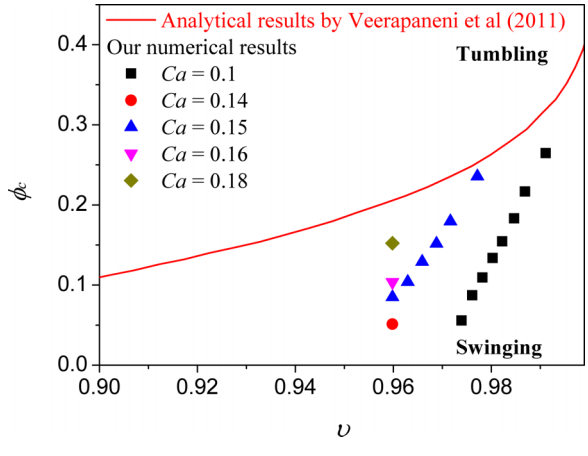

FIG. 7. Critical value of the inner capsule volume ratio (ϕ_c) versus the reduced volume υ for the swinging-to-tumbling transition of compound capsules. The solid line is the analytical result from the small-deformation theory by Veerapaneni *et al*. for compound vesicles enclosing a rigid particle. Here, the compound capsules are initially prolate.

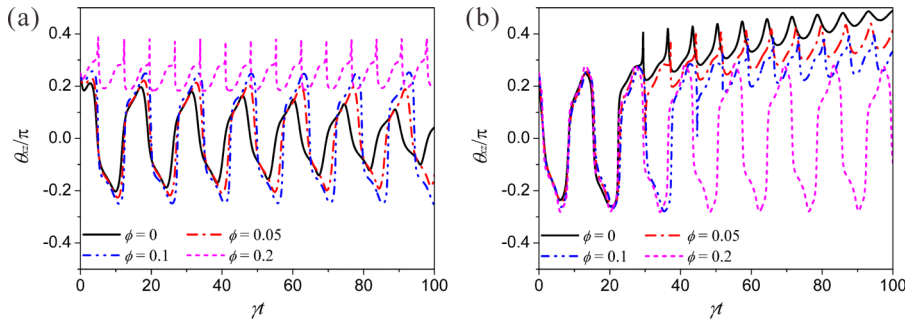

FIG. 8. Effects of the inner capsule on the dynamics of non-spherical compound capsules with the revolution axis initially off the shear plane. θ_{xz} is the angle between the revolution axis and its projection in the shear plane (i.e., x-z plane). Time evolutions of θ_{xz} are presented for oblate capsules with $a/b = 0.7$ (a) and prolate capsules with $a/b = 1.32$ (b), in which Ca is 0.1 and the initial value of θ_{xz} is $\pi/4$.

as shown in Figure 8, the homogeneous capsule with initially oblate shape presents the kayaking motion, in which the revolution axis oscillates back and forth symmetrically about the shear plane, while the prolate capsule presents the precession dynamics, in which the revolution axis makes a precessing motion about the vorticity axis (i.e., y axis) as it slowly drifts towards the vorticity axis. These specific motions have been revealed in previous numerical studies on homogeneous capsules.[45,46,48] As seen in Figure 8(a), with the volume ratio increasing to 0.1, the oblate compound capsule exhibits the kayaking motion, but the oscillating amplitude of the angle θ_{xz} between the revolution axis and its projection in the shear plane increases. As the volume ratio further increases to 0.2, the dynamical state of the oblate compound capsule changes to the stable precession dynamics, in which the revolution axis makes a stable precessing motion about the vorticity axis without drifting and hence θ_{xz} varies periodically about a constant mean. In Figure 8(b), with the volume ratio increasing, the prolate compound capsule initially presents the precession dynamics with drifting (its drifting speed is decreasing), and eventually the dynamical state changes to the kayaking motion. Previous studies on homogeneous capsules have demonstrated that many parameters, including the aspect ratio, capillary number, and viscosity ratio, can govern the off-plane motion of capsules.[45,46,48] The present study is limited to the cases of the fixed values of these parameters. Still it is noteworthy that the dynamical characteristics or rather the dynamical state of the off-plane motions can alternate by including an inner capsule and increasing its size.

IV. OBLATE COMPOUND CAPSULES WITH VISCOSITY MISMATCH

We first compare the dynamics of the prolate and oblate compound capsules. As shown in Figure 9, a significant difference in the dynamical characteristics is observed for the prolate and oblate compound capsules, even though they have the same reduced volume. In previous 3D simulations by Yazdani and Bagchi,[42] the same final shape of the homogeneous vesicles is presented for the same reduced volume, regardless of the initial shape of the vesicle (prolate or oblate). Our simulations indicate that the homogeneous capsules with the same reduced volume but with different initial shapes present much different dynamical characteristics (e.g., $\phi = 0$ in Figures 8(c) and 8(d)). Notably, Sui *et al*. reveal that the bending stiffness in the membrane is a key factor for the aforementioned phenomenon.[49] However, the differences in the dynamical characteristics are still observed in this study with the bending stiffness excluded (data not shown). Thus, we believe that the shear elasticity which is heavily dependent on the initial shape of capsules is another key factor. Regarding the compound capsules, at a given value of the inner capsule size, the oblate and prolate capsules also exhibit quite different behaviors. For example, the time evolutions of the lengths of the three principle axes are altered (Figure 8(a)) and the minimum values of both the deformation index and orientation angle are lower for the prolate capsules (Figures 9(c) and 9(d)). Besides, the critical inner capsule size for the swinging-to-tumbling transition is also lower for the prolate

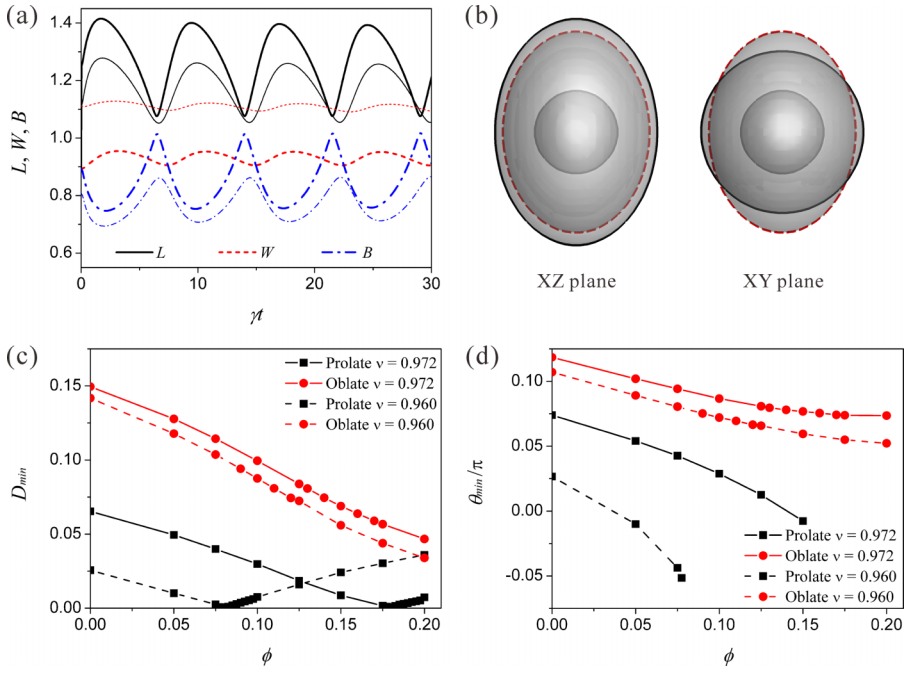

FIG. 9. Dynamics of ellipsoidal compound capsules: prolate versus oblate initial shapes. (a) Time evolutions of the three principal axes (thick lines for the prolate shape and thin lines for the oblate shape) and (b) the initial shape (black solid lines for the prolate shape and red dash lines for the oblate shape) of compound capsules at $\upsilon = 0.972$, $Ca = 0.15$, and $\phi = 0.1$. The minimum deformation index and the minimum orientation angle are plotted as functions of the volume ratio of the inner capsule in (c) and (d), respectively.

capsules. We believe that the presence of the spherical inner capsule is the reason for the differences in the dynamics between the prolate and oblate capsules apart from the shear elasticity of membranes. The inner and outer membranes are closer in the shear plane for the oblate compound capsules (Figure 9(b)), which may induce stronger hydrodynamic interactions.[30] In summary, the reduced volume, the only parameter used to define the shape effect in 2D simulations, is no longer sufficient in 3D situations. Therefore, a more native-mimicking 3D model is needed for studying the dynamics of non-spherical compound capsules, as the additional freedom in the third dimension brings more complex behaviors.

It is well known that the deformation and dynamics of homogeneous capsules are significantly affected by the viscosity mismatch between the internal and external fluids.[3,10,50] In our present work, we investigate the effects of the viscosity ratios (i.e., λ and λ^{in}) on the dynamics of compound capsules (Figure 10). With λ increasing at a given value of ϕ, the dynamical state of the compound capsules can change from swinging to tumbling, which is similar to the case for homogeneous capsules.[10,13] At the swinging-to-tumbling transition induced by increasing λ, the minimum value of the deformation index D_{min} becomes very close to zero (Figure 10(a)). For each group of λ and λ^{in}, D_{min} decreases with ϕ in the swinging regime (Figure 10(b)). Notably, D_{min} decreases significantly as λ increases with λ^{in} maintained constant at 1, whereas insignificant change is observed in D_{min} as λ^{in} increases from 1 to 3 with λ maintained constant at 1. In our previous work, it is observed that the deformation of spherical compound capsules also depends on the outer viscosity ratio more than on the inner viscosity ratio.[30] In Figure 9(c), the oscillation amplitude ΔD of the deformation index is found to increase first and then decrease with increasing λ in both the cases of the homogeneous and compound capsules. ΔD reaches its maximum at an intermediate value of λ when the swinging-to-tumbling transition occurs, and this intermediate value of λ decreases with ϕ. It is known that the swinging-to-tumbling transition occurs once the viscosity ratio exceeds a critical value. In Figure 10(d), the effects of the inner capsule size on the critical viscosity ratio are examined by presenting the phase diagram as a function of λ and ϕ. The critical viscosity ratio for

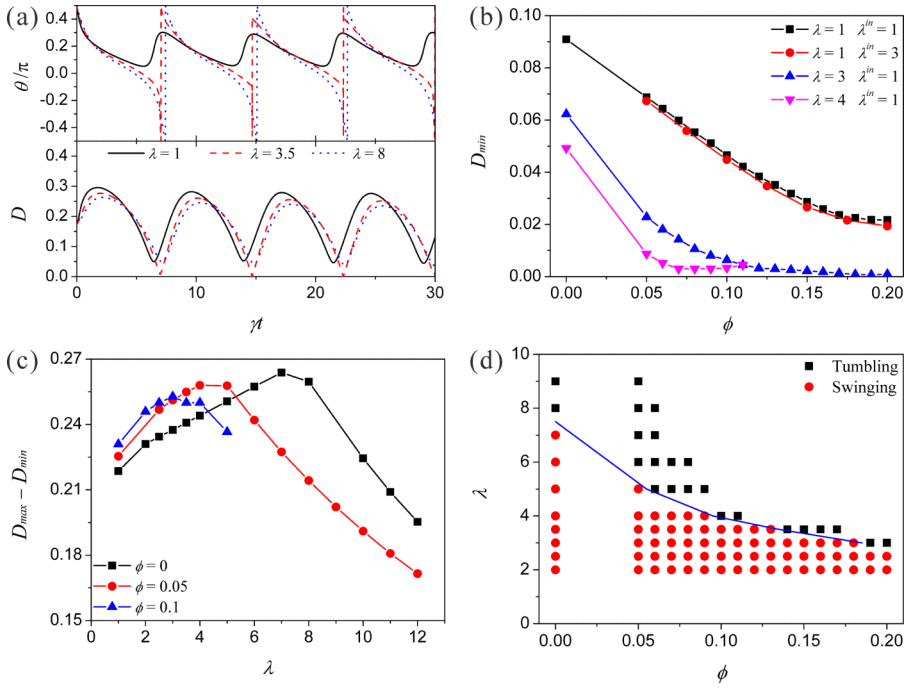

FIG. 10. Influences of the viscosity ratios λ and λ^{in} on the dynamics of compound capsules. (a) Time evolutions of the deformation index D and orientation angle θ for different λ at $a/b = 0.7$, $Ca = 0.1$, and $\phi = 0.1$. (b) The minimum value of the deformation index is plotted as a function of ϕ at different λ. (c) Oscillation amplitude $D_{max} - D_{min}$ of the deformation index is plotted as a function of λ at different ϕ. (d) Phase diagram as a function of ϕ and λ for $a/b = 0.7$ and $Ca = 0.1$.

the swinging-to-tumbling transition decreases significantly with the increasing ϕ, which means that the tumbling motion is facilitated by the presence of the inner capsule and the increase of its size. From this point of view, increasing the volume ratio of the inner capsule has a similar effect on the capsule dynamics as increasing the viscosity ratio.

V. DISCUSSIONS

In previous studies on the dynamics of compound vesicles, including the small deformation theory analysis for vesicles enclosing rigid particles[28] and 2D simulations for vesicles enclosing deformable vesicles,[29] the increase of the effective internal fluid viscosity induced by the presence of inclusions is proposed to explain the inclusion-induced tank-treading-to-tumbling transition. Our present study presents a discussion about the influences of the inner capsule on the effective viscosity of the inhomogeneous fluid inside the compound capsule to explore the mechanism of the effects of the inner capsule on the compound capsule dynamics.

With the calculation method for the effective viscosity of a dilute suspension of liquid-filled capsules modelled with the front-tracking method,[51] the effective viscosity of the inhomogeneous fluid inside the compound capsule (i.e., the outer capsule) is computed as follows:

$$\mu^* = \lambda\mu + \frac{\sigma_{xz}}{S_{xz}}. \tag{5.1}$$

Here, S_{xz} is the average shear rate in the compound capsule and σ_{xz} is the excess shear stress accounting for the contribution of the inner capsule. S_{xz} is calculated as follows:

$$S_{xz} = \frac{1}{V}\int_A (u_x n_z + u_z n_x)\, dA, \tag{5.2}$$

where V and A are the volume and surface area of the outer capsule, respectively, u_x and u_z are the X- and Z-component of the velocity vector, respectively, and n_x and n_z are the X- and Z-component

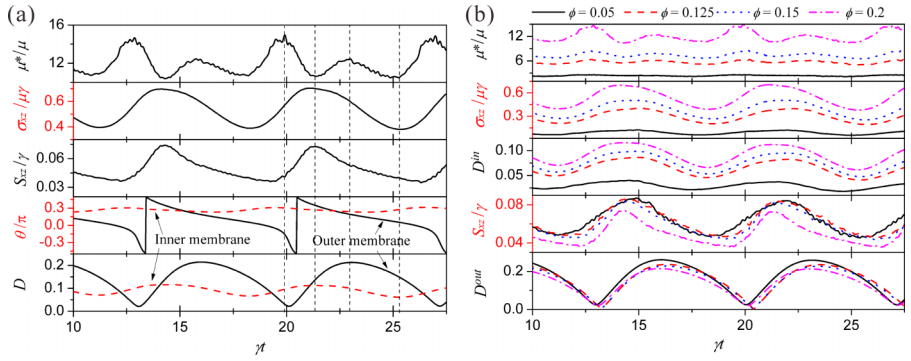

FIG. 11. (a) Time evolutions of the deformation index D, the orientation angle θ, the average shear rate S_{xz} inside the compound capsule, the excess shear stress σ_{xz} induced by the inner capsule, and the effective internal fluid viscosity μ^* for a tumbling compound capsule ($a/b = 1.32$, $\phi = 0.2$, and $Ca = 0.1$). (b) Time evolutions of D, S_{xz}, σ_{xz}, and μ^* at different ϕ when $a/b = 1.32$ and $Ca = 0.1$. The capsules with $\phi = 0.05$ and 0.125 exhibit the swinging motion and capsules with $\phi = 0.15$ and 0.2 exhibit the tumbling motion.

of the unit outward normal vector, respectively. σ_{xz} is calculated as follows:

$$\sigma_{xz} = \frac{1}{V^{in}} \int_{A^{in}} \left[f_x x_z + \mu\lambda \left(\lambda^{in} - 1\right)\left(u_x n_z + u_z n_x\right) \right] dA^{in}, \tag{5.3}$$

where V^{in} and A^{in} are the volume and surface area of the inner capsule, respectively, f is the elastic force in the capsule membrane, and x is the position of membrane points.

Figure 11 presents the time evolutions of the average shear rate S_{xz}, the excess shear stress σ_{xz}, and the effective internal fluid viscosity μ^* in dimensionless forms for compound capsules with different sizes of inner capsules. It is noted that S_{xz}, σ_{xz}, and μ^* are all time-dependent quantities regardless of the regime that the compound capsule is in the swinging or tumbling regime, as the capsule shape and orientation angle oscillate over time. The excess shear stress σ_{xz} primarily depends on the deformation of the inner capsule, while the average shear rate S_{xz} is affected by both the deformation and the orientation of the outer capsule. The non-Newtonian rheological behaviour of the compound capsule, i.e., the time-dependent internal fluid viscosity, is similar to the observations in previous 2D simulations for compound vesicles.[29] However, there are significant differences in the variations of S_{xz}, σ_{xz}, and μ^* versus time between our 3D simulations and the 2D simulations by Kaoui *et al.*[29] For example, in previous 2D simulations, the effective internal fluid viscosity is found to diverge to the limit of a solid medium at $\theta = \pm\pi/4$, but the same divergence is not observed in our 3D simulations as the average shear rate never approaches zero. Notably, owing to the presence of the inner membrane, the effective viscosity of the fluid inside the compound capsule increases significantly (i.e., $\mu^* > 10\mu$ for $\phi = 0.2$ in Figure 10(a)). As the volume ratio of the inner capsule increases, the outer capsule deformation decreases, but the inner capsule deformation increases due to the stronger hydrodynamic interaction between the inner and outer membranes.[30] Accordingly, the average shear rate decreases with the decreasing outer capsule deformation, which is also indicated in our previous study,[30] and the excess shear stress increases with the increasing inner capsule deformation. As a result, the effective internal fluid viscosity of compound capsules increases as the inner capsule is enlarged (Figure 11(b)).

Figure 12 shows that the time-averaged value of the effective internal fluid viscosity μ^*_{av} always increases with the increasing volume ratio ϕ of the inner capsule for different values of Ca and a/b. Previous theoretical analyses and 2D simulations for compound vesicles also conclude the increasing tendency of the effective internal fluid viscosity with the inclusion size.[28,29] In qualitative terms, the increase of μ^*_{av} versus ϕ can be used to address the effects of the inclusions on the dynamics of compound capsules. For example, increasing the inner capsule size alone can induce the swinging-to-tumbling transition at vanishing viscosity mismatch (Figure 2). The effective internal fluid viscosity also increases with the capillary number decreasing, which in qualitative terms is another reason for the increase of the critical volume ratio versus the capillary number (Figure 7).

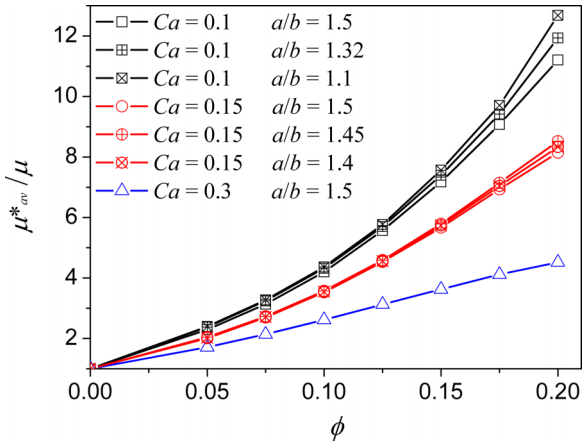

FIG. 12. Effective internal fluid viscosity is plotted as a function of ϕ at different a/b and Ca.

Note that decreasing the capillary number also facilitates the tumbling of homogeneous capsules due to the pronounced shape memory effect.[9,10]

However, in quantitative terms, compound capsules do not exhibit exactly the same dynamical behaviors as homogeneous capsules, even if the effective internal fluid viscosity of compound capsules is the same as the internal viscosity of homogeneous capsules. The minimum deformation index D_{min} and orientation angle θ_{min} are used to predict the transition of dynamical states in our 3D simulations and in previous 2D simulations,[28,29] respectively. Thus, we plot D_{min} and θ_{min} of compound capsules versus μ^*_{av}/μ in Figure 13, in which D_{min} and θ_{min} of homogeneous capsules versus λ^H are also plotted for the comparison purpose. In the swinging regime, both D_{min} and θ_{min} decrease with μ^*_{av}/μ for compound capsules, which is qualitatively similar to those of homogeneous capsules versus λ^H. Notably, the decreasing of θ_{min} for compound capsules at $\lambda = 1$ is gradually decelerated with μ^*_{av}/μ, while it is accelerated for homogeneous capsules. Besides, θ_{min} of compound capsules is larger than that of homogeneous capsules, in the case of low outer viscosity ratio (i.e., $\lambda = 1$) in particular. Moreover, D_{min} of compound capsules is also inconsistent with that of homogeneous capsules. The decreasing speed of D_{min} near the swinging-to-tumbling transition for compound capsules is much lower than that of homogeneous capsules, and the transition is thus delayed, i.e., the critical $\mu^*_{av}/\mu = 8.35$ for compound capsules is higher than the critical

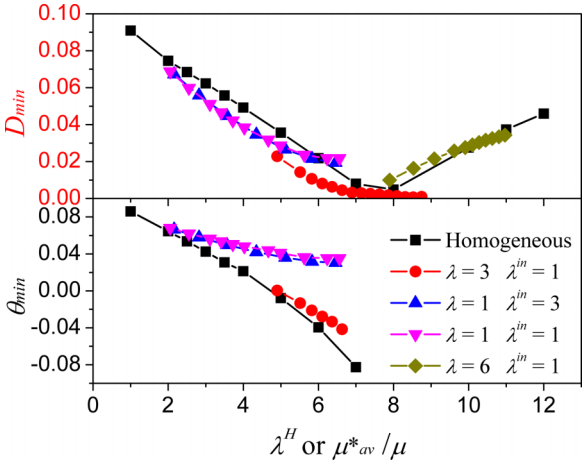

FIG. 13. The minimum values of the deformation index D_{min} and the orientation angle θ_{min} are plotted as functions of the time-average value of the effective viscosity ratio μ^*_{av}/μ for compound capsules with $a/b = 0.7$ and $Ca = 0.1$. Corresponding values of homogeneous capsules versus the viscosity ratio λ^H are also presented for the comparison purpose.

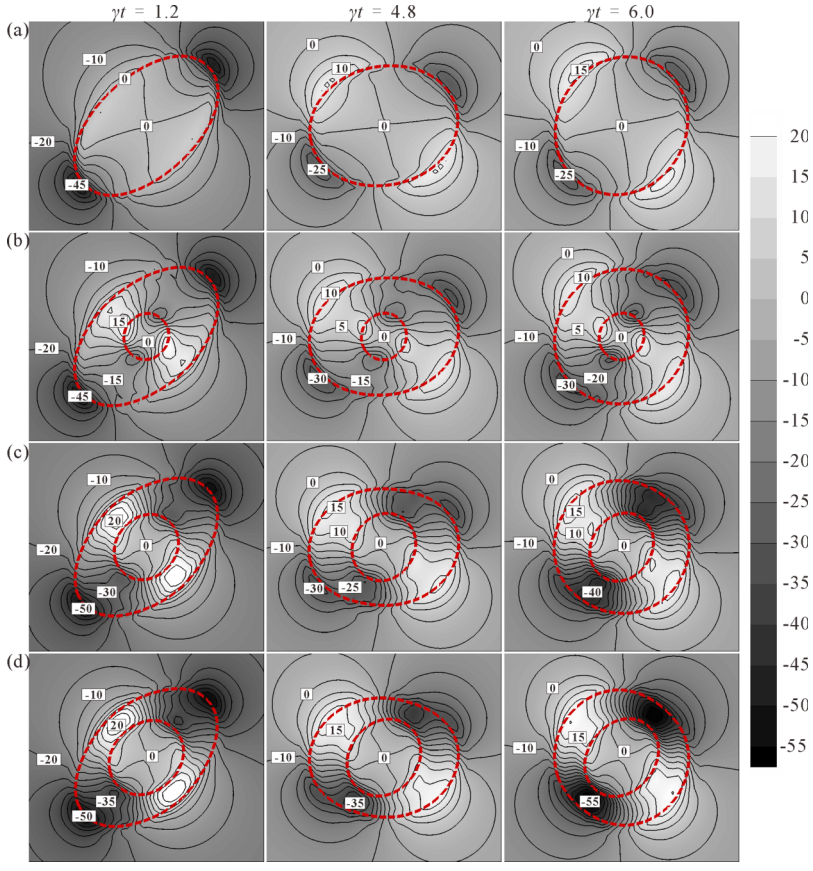

FIG. 14. Dimensionless pressure field $p/\rho R^2\gamma^2$ inside and outside the capsules with $a/b = 1.32$, $Ca = 0.1$, and $\lambda = \lambda^{in} = 1$. (a) $\phi = 0$ in the swinging regime with $D_{min} = 0.035$. (b) $\phi = 0.05$ in the swinging regime with $D_{min} = 0.0249$. (c) $\phi = 0.135$ at the swinging-tumbling transition with $D_{min} = 0.0005$. (d) $\phi = 0.2$ in the tumbling regime with $D_{min} = 0.0221$. The pressure values are relative deviations from pressure at the center point of the capsule.

$\lambda^H = 7.58$. Under certain conditions (e.g., $\lambda = \lambda^{in} = 1$), the swinging-to-tumbling transition for the compound capsule will not occur by increasing the inner capsule size alone, though the effective viscosity contrast increases to high values. Kaoui *et al.*[29] also observe that the orientation angle of compound vesicles is larger than that of homogeneous vesicles, though they report the critical value of μ^*_{av}/μ for the tank-treading-to-tumbling transition of compound vesicles is close to the critical viscosity contrast of homogeneous vesicles.

Figure 14 shows the inhomogeneous distribution of fluid stresses inside the compound capsule due to the hydrodynamic interaction between the inner and outer membranes. Our previous work on spherical compound capsules concludes that the hydrodynamic interaction can be largely reflected by the pressure distribution.[30] Similarly, a pressure gradient directed from the capsule equator to the tip is also observed in the fluid layer between the two membranes of the nonspherical compound capsules. This pressure gradient increases with the inner capsule size; as a result, the compound capsule deformation decreases (Figures 5(a) and 5(b)), which is also observed for spherical compound capsules. Notably, as the outer capsule tumbles or swings versus time, the higher pressure region is always near the equator of the inner capsule (Figures 14(b)–14(d)). In contrast, the high pressure region can appear near the tip of the outer capsule when the major axis of the outer capsule tumbles to be perpendicular to that of the inner capsule (Figures 14(c) and 14(d)). Under this specific condition, the pressure gradient prevents the initially nonspherical outer capsule from deforming to be spherical. It is the likely reason for the fact that the minimum deformation of the tumbling compound capsules increases with the inner capsule size (Figures 5(c) and 5(d)). As shown in Figures 14(b)–14(d), compared to that inside the inner capsule, the pressure between the

two membranes is much higher near the capsule equator but is much lower near the capsule tip. Apparently, highly inhomogeneous distribution of pressure results from the presence of the inner membrane, especially at high volume ratios of the inner capsule. These findings further indicate that compound capsules cannot be viewed as homogeneous capsules in the study on their motions in shear flow.

VI. CONCLUSIONS

In this study, we numerically investigate the dynamics of a nonspherical compound capsule (a prolate/oblate capsule containing a smaller spherical capsule) in simple shear flow by using a three-dimensional front-tracking finite-difference model. In this model, the shear elasticity, area dilatation, and bending resistance are considered for the discovery of the membrane mechanics. Our main findings are concluded as follows:

(1) Compound capsules exhibit the same swinging and tumbling motions as homogeneous capsules do, and the phase diagram for their occurrence is presented. The swinging-to-tumbling transition can be induced at vanishing viscosity contrast by increasing the inner capsule size alone. The critical inner capsule size for the swinging-to-tumbling transition increases with the capillary number and the reduced volume. Compared to previous small deformation theories, our numerical model is more applicable when the capillary number is high or the reduced volume is low. Further, increasing the inner capsule size leads to the significant decrease of the critical viscosity ratio for the swinging-to-tumbling transition for compound capsules with viscosity contrast.

(2) The presence of the inner capsule and increasing its size significantly affect the dynamical characteristics of both the swinging and tumbling motions, such as the time-average and minimum values of the deformation index and orientation angle. Particularly, as the inner capsule size increases, the minimum deformation index decreases in the swinging regime but increases in the tumbling regime. At the swinging-to-tumbling transition, the compound capsule transforms to be circular in the shear plane, while in three dimensions it is oblate with the revolution axis in the vorticity direction.

(3) The mechanisms underlying the effects of the inner capsule on the compound capsule dynamics are discovered. Owing to the presence of the inner capsule, the effective viscosity of the fluid inside the compound capsule is enlarged and it increases with the inner capsule size, which accounts for the swinging-to-tumbling transition induced by increasing the inner capsule size in qualitative terms. However, in quantitative terms, compound capsules do not exhibit exactly the same behaviors as homogeneous capsules, as the presence of the inner membrane induces significant inhomogeneity of fluid stress distribution inside the compound capsule.

Our present research findings provide new insights into the motion of elastic capsules in shear flow which have not been thoroughly examined to our best knowledge. Nevertheless, there are still numerous issues to address in future work regarding the practical application of the fundamental research findings, for instance, the extremely large volume ratio of the inner to outer capsules, the extremely high viscosity and the viscoelastic nature of internal fluids for biological compound capsules, more complicated mechanical properties of the capsule membrane including viscoelasticity and extremely high area-dilatation modulus.

ACKNOWLEDGMENTS

This work was supported by the China National Funds for Distinguished Young Scientists (Grant No. 51425603).

[1] D. Barthes-Biesel, "Capsule motion in flow: Deformation and membrane buckling," C. R. Phys. **10**, 764–774 (2009).
[2] D. Barthes-Biesel, "Modeling the motion of capsules in flow," Curr. Opin. Colloid Interface Sci. **16**, 3–12 (2011).
[3] D. Barthes-Biesel, "Motion and deformation of elastic capsules and vesicles in flow," Annu. Rev. Fluid Mech. **48**, 25–52 (2016).

[4] M. P. Neubauer, M. Poehlmann, and A. Fery, "Microcapsule mechanics: From stability to function," Adv. Colloid Interface Sci. **207**, 65–80 (2014).
[5] R. Finken, S. Kessler, and U. Seifert, "Micro-capsules in shear flow," J. Phys.: Condens. Matter **23**, 184113 (2011).
[6] T. M. Fischer, "Shape memory of human red blood cells," Biophys. J. **86**, 3304–3313 (2004).
[7] J. M. Skotheim and T. W. Secomb, "Red blood cells and other nonspherical capsules in shear flow: Oscillatory dynamics and the tank-treading-to-tumbling transition," Phys. Rev. Lett. **98**, 078301 (2007).
[8] Y. Sui, H. T. Low, Y. T. Chew, and P. Roy, "Tank-treading, swinging, and tumbling of liquid-filled elastic capsules in shear flow," Phys. Rev. E **77**, 016310 (2008).
[9] P. M. Vlahovska, Y. N. Young, G. Danker, and C. Misbah, "Dynamics of a non-spherical microcapsule with incompressible interface in shear flow," J. Fluid Mech. **678**, 221–247 (2011).
[10] P. Bagchi and R. M. Kalluri, "Dynamics of nonspherical capsules in shear flow," Phys. Rev. E **80**, 016307 (2009).
[11] S. Ramanujan and C. Pozrikidis, "Deformation of liquid capsules enclosed by elastic membranes in simple shear flow: Large deformations and the effect of fluid viscosities," J. Fluid Mech. **361**, 117–143 (1998).
[12] D. V. Le, "Effect of bending stiffness on the deformation of liquid capsules enclosed by thin shells in shear flow," Phys. Rev. E **82**, 016318 (2010).
[13] J. Walter, A. V. Salsac, and D. Barthes-Biesel, "Ellipsoidal capsules in simple shear flow: Prolate versus oblate initial shapes," J. Fluid Mech. **676**, 318–347 (2011).
[14] D. V. Le and S. T. Wong, "A front-tracking method with Catmull-Clark subdivision surfaces for studying liquid capsules enclosed by thin shells in shear flow," J. Comput. Phys. **230**, 3538–3555 (2011).
[15] H. Noguchi, "Dynamic modes of microcapsules in steady shear flow: Effects of bending and shear elasticities," Phys. Rev. E **81**, 056319 (2010).
[16] A. Yazdani and P. Bagchi, "Influence of membrane viscosity on capsule dynamics in shear flow," J. Fluid Mech. **718**, 569–595 (2013).
[17] A. Z. K. Yazdani and P. Bagchi, "Phase diagram and breathing dynamics of a single red blood cell and a biconcave capsule in dilute shear flow," Phys. Rev. E **84**, 026314 (2011).
[18] D. A. Fedosov, B. Caswell, and G. E. Karniadakis, "A multiscale red blood cell model with accurate mechanics, rheology, and dynamics," Biophys. J. **98**, 2215–2225 (2010).
[19] L.-Y. Chu, A. S. Utada, R. K. Shah, J.-W. Kim, and D. A. Weitz, "Controllable monodisperse multiple emulsions," Angew. Chem., Int. Ed. **46**, 8970–8974 (2007).
[20] H. A. Stone and L. G. Leal, "Breakup of concentric double emulsion droplets in linear flows," J. Fluid Mech. **211**, 123–156 (1990).
[21] K. A. Smith, J. M. Ottino, and M. O. de la Cruz, "Encapsulated drop breakup in shear flow," Phys. Rev. Lett. **93**, 204501 (2004).
[22] S. Patlazhan, S. Vagner, and I. Kravchenko, "Steady-state deformation behavior of confined composite droplets under shear flow," Phys. Rev. E **91**, 063002 (2015).
[23] Y. Chen, X. Liu, and Y. Zhao, "Deformation dynamics of double emulsion droplet under shear," Appl. Phys. Lett. **106**, 141601 (2015).
[24] J. Wang, J. Liu, J. Han, and J. Guan, "Effects of complex internal structures on rheology of multiple emulsions particles in 2D from a boundary integral method," Phys. Rev. Lett. **110**, 066001 (2013).
[25] M. Levant and V. Steinberg, "Complex dynamics of compound vesicles in linear flow," Phys. Rev. Lett. **112**, 138106 (2014).
[26] A. Pommella, S. Caserta, V. Guida, and S. Guido, "Shear-induced deformation of surfactant multilamellar vesicles," Phys. Rev. Lett. **108**, 138301 (2012).
[27] A. Pommella, S. Caserta, and S. Guido, "Dynamic flow behaviour of surfactant vesicles under shear flow: Role of a multi-lamellar microstructure," Soft Matter **9**, 7545–7552 (2013).
[28] S. K. Veerapaneni, Y. N. Young, P. M. Vlahovska, and J. Blawzdziewicz, "Dynamics of a compound vesicle in shear flow," Phys. Rev. Lett. **106**, 158103 (2011).
[29] B. Kaoui, T. Kruger, and J. Harting, "Complex dynamics of a bilamellar vesicle as a simple model for leukocytes," Soft Matter **9**, 8057–8061 (2013).
[30] Z. Y. Luo, L. He, and B. F. Bai, "Deformation of spherical compound capsules in simple shear flow," J. Fluid Mech. **775**, 77–104 (2015).
[31] R. Skalak, A. Tozeren, R. P. Zarda, and S. Chien, "Strain energy function of red blood cell membranes," Biophys. J. **13**, 245–280 (1973).
[32] W. Helfrich, "Elastic properties of lipid bilayers: Theory and possible experiments," Z. Naturforsch. C **28**, 693–703 (1973).
[33] O. Y. Zhongcan and W. Helfrich, "Bending energy of vesicle membranes: General expressions for the first, second, and third variation of the shape energy and applications to spheres and cylinders," Phys. Rev. A **39**, 5280–5288 (1989).
[34] C. Pozrikidis, "Effect of membrane bending stiffness on the deformation of capsules in simple shear flow," J. Fluid Mech. **440**, 269–291 (2001).
[35] C. Dupont, A. V. Salsac, D. Barthes-Biesel, M. Vidrascu, and P. Le Tallec, "Influence of bending resistance on the dynamics of a spherical capsule in shear flow," Phys. Fluids **27**, 051902 (2015).
[36] D. Barthes-Biesel, A. Diaz, and E. Dhenin, "Effect of constitutive laws for two-dimensional membranes on flow-induced capsule deformation," J. Fluid Mech. **460**, 211–222 (2002).
[37] X. J. Li, P. M. Vlahovska, and G. E. Karniadakis, "Continuum- and particle-based modeling of shapes and dynamics of red blood cells in health and disease," Soft Matter **9**, 28–37 (2013).
[38] Z. Y. Luo, S. Q. Wang, L. He, F. Xu, and B. F. Bai, "Inertia-dependent dynamics of three-dimensional vesicles and red blood cells in shear flow," Soft Matter **9**, 9651–9660 (2013).
[39] Z. Y. Luo and B. F. Bai, "Dynamics of biconcave vesicles in a confined shear flow," Chem. Eng. Sci. **137**, 548–555 (2015).
[40] G. Tryggvason, B. Bunner, A. Esmaeeli, D. Juric, N. Al-Rawahi, W. Tauber, J. Han, S. Nas, and Y. J. Jan, "A front-tracking method for the computations of multiphase flow," J. Comput. Phys. **169**, 708–759 (2001).

[41] X. Y. Li and K. Sarkar, "Front tracking simulation of deformation and buckling instability of a liquid capsule enclosed by an elastic membrane," J. Comput. Phys. **227**, 4998–5018 (2008).
[42] A. Yazdani and P. Bagchi, "Three-dimensional numerical simulation of vesicle dynamics using a front-tracking method," Phys. Rev. E **85**, 056308 (2012).
[43] S. Shrivastava and J. Tang, "Large deformation finite element analysis of non-linear viscoelastic membranes with reference to thermoforming," J. Strain Anal. Eng. **28**, 31–51 (1993).
[44] M. Y. Zhao and P. Bagchi, "Dynamics of microcapsules in oscillating shear flow," Phys. Fluids **23**, 111901 (2011).
[45] D. Cordasco and P. Bagchi, "Orbital drift of capsules and red blood cells in shear flow," Phys. Fluids **25**, 091902 (2013).
[46] C. Dupont, A. V. Salsac, and D. Barthes-Biesel, "Off-plane motion of a prolate capsule in shear flow," J. Fluid Mech. **721**, 180–198 (2013).
[47] Z. Y. Luo, L. He, F. Xu, and B. F. Bai, "Three-dimensional numerical simulation of vesicle dynamics in microscale shear flows," J. Nanosci. Nanotechnol. **15**, 3081–3086 (2015).
[48] Z. Wang, Y. Sui, P. D. M. Spelt, and W. Wang, "Three-dimensional dynamics of oblate and prolate capsules in shear flow," Phys. Rev. E **88**, 053021 (2013).
[49] Y. Sui, Y. T. Chew, P. Roy, X. B. Chen, and H. T. Low, "Transient deformation of elastic capsules in shear flow: Effect of membrane bending stiffness," Phys. Rev. E **75**, 066301 (2007).
[50] E. Foessel, J. Walter, A. V. Salsac, and D. Barthes-Biesel, "Influence of internal viscosity on the large deformation and buckling of a spherical capsule in a simple shear flow," J. Fluid Mech. **672**, 477–486 (2011).
[51] P. Bagchi and R. M. Kalluri, "Rheology of a dilute suspension of liquid-filled elastic capsules," Phys. Rev. E **81**, 056320 (2010).